DOI 10.1007/s00702-004-0181-4
J Neural Transm (2005) 112: 269–282

Journal of Neural Transmission
Printed in Austria

Amelioration of the cerebrovascular amyloidosis in a transgenic model of Alzheimer's disease with the neurotrophic compound Cerebrolysin™

E. Rockenstein[1], **A. Adame**[1], **M. Mante**[1], **G. Larrea**[1], **L. Crews**[1], **M. Windisch**[3], **H. Moessler**[4], and **E. Masliah**[1,2]

[1] Department of Neurosciences, and
[2] Department of Pathology, University of California, San Diego School of Medicine, La Jolla, CA, USA
[3] JSW-RESEARCH, Graz, and
[4] EBEWE Pharmaceuticals Research Division, Unterach, Austria

Received February 8, 2004; accepted May 11, 2004
Published online July 7, 2004;

Summary. Increased production and reduced clearance of amyloid β (Aβ) plays a central role in the pathogenesis of Alzheimer's disease (AD). We have recently shown that the neurotrophic peptide mixture Cerebrolysin™ (Cbl) has the ability of improving synaptic functioning and reducing amyloid deposition in a transgenic (tg) animal model of Alzheimer's disease (AD). Since in AD, potentially toxic Aβ aggregates accumulate not only around neurons but also in the blood vessels, then it is important to investigate whether bioactive compounds such as Cbl might have the capacity to ameliorate the age-related cerebral amyloid angiopathy (CAA) in tg models. To this end, tg mice expressing mutant human amyloid precursor protein (APP) under the Thy1 promoter were treated with Cbl or saline alone starting at 7 or 12 months of age for a total of three months. Neuropathological analysis with an antibody against Aβ showed that Cbl decreased amyloid deposition around the blood vessels in a time dependant manner. These effects were accompanied by a reduction in perivascular microgliosis and astrogliosis and increased expression of markers of vascular fitness such as CD31 and ZO-1. No lymphocytic infiltration was observed associated with Aβ in the vessels. Consistent with these findings, ultrastructural analysis showed that while in tg mice treated with saline alone there was an abundant accumulation of amyloid fibers in the vascular wall accompanied by thickening of the basal membrane and endothelial cell damage, in Cbl-treated mice there was considerable reduction in the subcellular alterations of endothelial and smooth muscle cells with preservation of basal membranes and intercellular junctions. Taken together, these results suggest that Cbl treatment might have beneficial effects in patients with cognitive impairment due to

cerebrovascular amyloidosis by reducing Aβ accumulation and promoting the preservation of the cerebrovasculature.

Keywords: Alzheimer's, amyloid-β, Cerebrolysin, cerebral amyloid angiopathy, cerebrovascular.

Introduction

Abnormal processing of amyloid precursor protein (APP) leading to increased amyloid beta protein (Aβ) production has been centrally implicated in the pathogenesis of Alzheimer's disease (AD) because APP mutations are associated with familial AD (FAD) (Goate et al., 1991; Clark and Goate, 1993), APP degradation products are found in AD brains (Sisodia et al., 1990), and over expression of mutated APP in transgenic (tg) mice results in AD-like pathology (Games et al., 1995). Cleavage of APP by α-secretase results in the secretion of a large N-terminal ectodomain (Maruyama et al., 1994). In an alternative pathway, β-secretase generates a shorter N-terminal fragment and a 12-kDa C-terminal fragment (C99), which remains membrane bound (Evin et al., 2003). C99 is then further cleaved by γ-secretase, resulting in the production of Aβ peptides (Beher et al., 2002; Evin et al., 2003). These fragments accumulate in the neurons as well as at the synaptic sites triggering pro-apoptotic pathways (Mattson, 2000; Bertrand et al., 2001; Mattson et al., 2001; Lu et al., 2003a, b). Furthermore, fibrillar Aβ peptides accumulate in the extracellular space forming plaques and around blood vessels leading to cerebral amyloid angiopathy (CAA). CAA is a common feature of both sporadic and FAD where amyloid is found around arteries, arterioles and less often around capillaries and veins (Revesz et al., 2002). Immunocytochemical studies have shown that Aβ1-40 is the predominant form of Aβ accumulating in the blood vessels in sporadic AD, while in FAD Aβ1-42 is also deposited (Revesz et al., 2002). Although Aβ peptides are primarily deposited as amyloid in CAA, monomeric and oligomeric forms of this peptide are also found. In cases with moderate to severe forms of CAA there is a significantly higher frequency of hemorrhagic or ischemic lesions contributing to the worsening of the cognitive impairment in these patients (Revesz et al., 2002; Van Nostrand et al., 2002; Weller and Nicoll, 2003). Thus, developing strategies directed at reducing cerebrovascular amyloidosis and protecting the microvasculature might be an important adjuvant therapy in patients with AD.

In this regard, previous studies have shown that Cerebrolysin™ (Cbl), a brain derived peptide preparation produced by a standardized enzymatic breakdown of purified brain proteins, has neurotrophic activity *in vitro* (Mallory et al., 1999) and in animal models of cerebrovascular ischemia and neurodegeneration (Francis-Turner and Valouskova, 1996; Masliah et al., 1999; Veinbergs et al., 2000) and improves the memory deficits in patients with mild to moderate AD (Ruther et al., 1994a, b) and after stroke (Koppi and Barolin, 1998). Furthermore, we recently found that this compound is capable of reducing amyloid load and neurodegeneration in APP tg mice expressing mutated human (h)APP751 under the control of the murine (m)Thy-1 promoter (mThy1-hAPP751) (Rockenstein et al., 2002). Because the mutations introduced in this APP tg mouse model are

the same as the ones associated with FAD (Chartier-Harlin et al., 1991; Clark and Goate, 1993), then this model might be more relevant to inherited than sporadic forms of AD. However, it is worth noting that since in both sporadic and FAD the same upstream event (Aβ1-42 accumulation) plays a central role in the pathogenesis of synaptic dysfunction and CAA (Haass et al., 1995; Citron et al., 1996; Mucke et al., 2000), then the findings in this model might be useful for both forms of AD. The advantages and disadvantages of the use of APP tg mouse models for the study of AD pathogenesis are discussed in recent review papers (Masliah, 1999; Masliah and Rockenstein, 2000).

Our previous studies were focused at investigating the effects of Cbl on plaque formation and neurodegeneration in mThy1-hAPP751 tg mice, however, it is unclear if Cbl might have similar effects in CAA. Therefore, in the present study, we evaluated the effects of Cbl on Aβ deposition in the vessels and on vascular fitness.

Material and methods

Generation of mThy1-hAPP751 tg mice and treatment regimen

Briefly, as previously described (Rockenstein et al., 2001), the tg mice generated for these studies express high levels of mutated hAPP751 under the control of the mThy-1 promoter (mThy1-hAPP751). These tg mice are unique in that, compared to other single tg models, high levels of Aβ1-42 are associated with amyloid plaque formation in the CNS at a much earlier age (beginning at 3 months) (Masliah and Rockenstein, 2000; Rockenstein et al., 2001). Furthermore, these mice develop CAA beginning at 6 months of age. Genomic DNA was extracted from tail biopsies and analyzed by PCR amplification, as described previously (Rockenstein et al., 1995). Transgenic lines were maintained by crossing heterozygous tg mice with non-transgenic (nontg) C57BL/6 × Swiss Webster F1 breeders. All mice were heterozygous with respect to the transgene and the nontg littermates served as controls. Twelve 7-month-old and twelve 12-month-old tg mice were utilized for the present study. For the younger age group (Group I), 6 mice received daily intraperitoneal (IP) injections of Cbl (Batch # 802772, 5 ml/kg) and the rest (n = 6) received saline alone. For the older age group (Group II), 6 tg mice received daily IP injections of Cbl (Batch # 802772, 5 ml/kg) and the rest (n = 6) received saline alone. Mice from each age group received IP injections for 1 month, followed by a month of rest and then another month of treatment. At the end of this 3 month period mice were sacrificed for neuropathological analysis. Thus, mice from Group I were sacrificed at 10 months of age and from Group II at 15 months of age.

Tissue processing

In accordance with NIH guidelines for the humane treatment of animals, mice were anesthetized with chloral hydrate and flush-perfused transcardially with 0.9% saline. Brains were removed and divided sagitally. One hemibrain was post-fixed in phosphate-buffered 4% paraformaldehyde (pH 7.4) at 4°C for 48 hr and sectioned at 40-μm with a Vibratome 2000 (Leica, Nussloch, Germany), while the other hemibrain was snap frozen and stored at −70°C for protein analysis.

Neuropathological analysis and detection of Aβ deposits

Vibratome sections were incubated overnight at 4°C with the mouse monoclonal antibody against Aβ protein (clone 6E10, 1:600, Signet Labs, Inc., Dedham, MA), followed by fluorescein isothiocyanate (FITC)-conjugated anti-mouse IgG (1:75, Vector Laboratories, Burlingame, CA). The FITC-labeled sections were imaged with the laser scanning confocal microscope (LSCM, BioRad 1024; BioRad Laboratories, Hercules, CA), as described previously (Mucke et al., 2000). From each case a total of 10 digital images (0.1 mm^2) from the frontal cortex were analyzed to

determine the percent area occupied by interstitial amyloid deposits and CAA score. A semi-quantitative scale ranging from 0–3 was used to score the severity of the CAA (Wyss-Coray et al., 1997) in each image. A score of 0 = no amyloid deposition in vessels, 1 = approximately 1 to 4 vessels showing amyloid deposits, 2 = amyloid deposits in 5 to 9 vessels and 3 = 10 to 15 vessels with amyloid deposition. Additional analysis of the neuroinflammatory response and vascular alterations in the mThy1-hAPP751 tg mice was performed in sections immunolabeled with the antibody against glial fibrillary acidic protein (GFAP, 1:500, Chemicon, Temecula, CA), a marker of astroglial cells (Mucke et al., 2000), Iba1 (1:2000, Wako Chemicals USA, Inc., Richmond, VA), a microglial marker (Kanazawa et al., 2002) and with antibodies against CD3 (undiluted, R&D Systems, Minneapolis, MN), a T cell marker, CD20 (1:250, DakoCytomation, Carpinteria, CA), a B cell marker, CD31 (1:200, DakoCytomation) and ZO-1 (1:500, Chemicon) to determine patterns of vascular damage and preservation. Sections reacted with diaminobenzidine (DAB)/H_2O_2 were examined with a 20× objective of the Olympus light microscope. Digitized images were analyzed with the Quantimet 570C (Leica) to determine relative levels of vascular immunoreactivity (optical density). For all experiments, three immunolabeled sections were analyzed per mouse and the average of individual measurements was used to calculate group means.

Electron microscopic studies of CAA

For ultrastructural analysis, vibratome sections were postfixed with 2% glutaraldehyde/0.1% osmium tetroxide in 0.1 M sodium cacodylate buffer and fragments from the frontal cortex were embedded in Epoxy. Blocks were sectioned with an Ultracut E ultramicrotome (Leica) and analyzed with a Zeiss EM10 electron microscope (Carl Zeiss, Oberkochen, Germany) (Rockenstein et al., 2001). From each case a total of 20 electron micrographs were obtained, 10 at a final magnification of 5000x and 10 at 15,000x. Digitized micrographs of the vessels were used to determine the thickness of the basal membranes and percent area occupied by endothelial cells in small arterioles (Wyss-Coray et al., 2000).

Statistical analysis

Analyses were carried out with the StatView 5.0 program (SAS Institute Inc., Cary, NC). Differences among means were assessed by one-way ANOVA with post-hoc Dunnett's. Comparisons between 2 groups were done with the two-tailed unpaired Student's t-test. Correlation studies were carried out by simple regression analysis and the null hypothesis was rejected at the 0.05 level.

Fig. 1. Age-dependent patterns of amyloid deposition in the microvasculature in mThy1-hAPP751 tg mice. Sections were immunolabeled with an antibody against Aβ and analyzed with the LSCM. Panels **A**–**C** are from 7 month old mice and **D**–**F** are from 12 month old mice. **A**, **C** Amyloid angiopathy in the pial surface vessels in the frontal cortex. **B**, **D** Amyloid deposition in the vessels in the hippocampal fissure. **C**, **E** Amyloid involvement in the vessels in the thalamus. *PS* pial surface, *BV* blood vessel, *HF* hippocampal fissure, *P* plaque, Bar = 20 μm

Fig. 2. Effects of Cbl on CAA in mThy1-hAPP751 tg mice. Sections were immunolabeled with an antibody against Aβ and analyzed with the LSCM. All images are from the frontal cortex. **A** Nontg control displaying unaffected blood vessels. **B** Saline-treated tg mice from Group I (mice that started treatment at 7 months of age and were sacrificed at 10 months of age) display moderate amyloid deposition in vessels of small and intermediate caliber. **C** Saline-treated tg mice from Group II (mice that started treatment at 12 months of age and were sacrificed at 15 months of age) display abundant amyloid deposition in vessels of small and intermediate caliber. **D** Cbl-treated nontg control. **E**, **F** Cbl-treated mice from Groups I and II, respectively, display reduction of CAA and only occasional and compact plaques in the neuropil. *P* plaque, *BV* blood vessel, Bar = 20 μm

Results

Effects of Cbl treatment in the CAA in mThy1-hAPP751 tg mice

As expected, saline-treated mThy1-hAPP751 tg mice developed a progressively more severe age-related CAA (Fig. 1) compared to age matched nontg controls (Fig. 2A, D). Abundant amyloid deposits were frequently found in larger

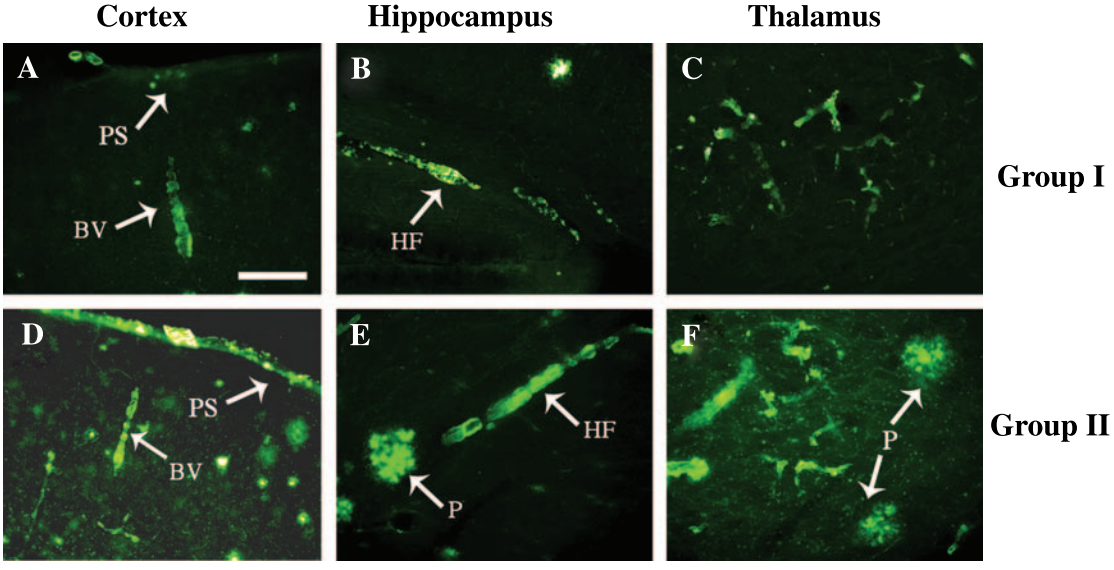

Fig. 1

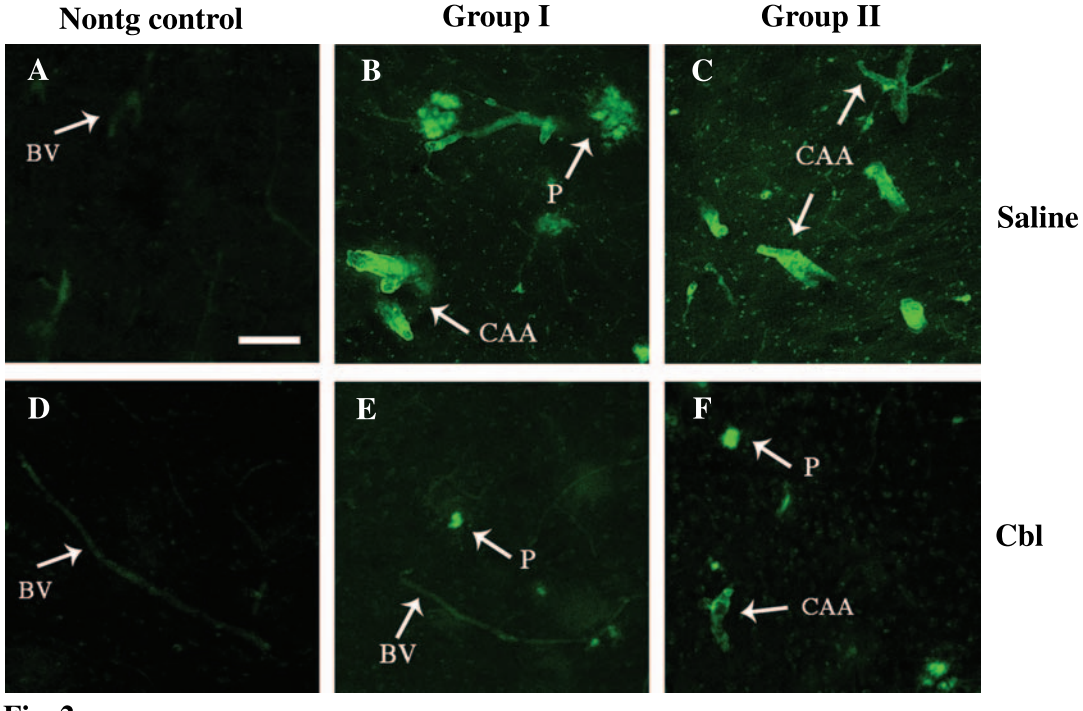

Fig. 2

vessels in the cortical pial surface (Fig. 1A, D; Fig. 2B, C) as well as in smaller vessels in the hippocampus and thalamus (Fig. 1C, F). In addition, abundant mature and diffuse plaques were found in the neuropil of these mice (Fig. 1D–F). In contrast, in tg mice treated with Cbl there was a considerable reduction in the scores for CAA (Fig. 2E, F; Fig. 3A) and interstitial amyloid deposits

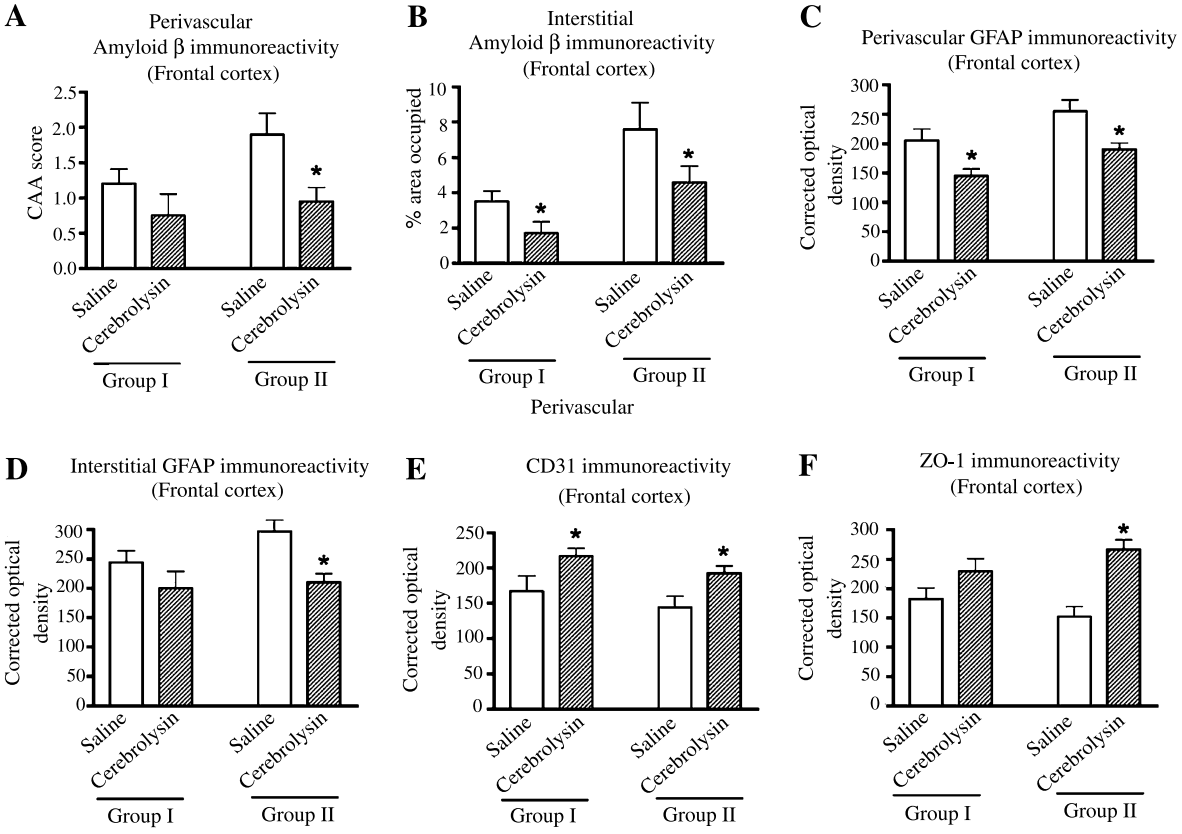

Fig. 3. Computer-aided image analysis of the cerebrovascular pathology in Cbl-treated mThy1-hAPP751 tg mice. Group I consisted of 7 month old mice treated with daily injections of Cbl over a 3 month period, and Group II consisted of 12 month old mice subjected to the same treatment procedure. All levels are measured in the frontal cortex. **A** Perivascular Aβ immunoreactivity expressed as CAA score. Cbl treatment reduced CAA in both Group I and Group II, but most significantly in Group II. **B** Levels of interstitial Aβ immunoreactivity expressed as percent area of the neuropil occupied by diffuse and mature amyloid plaques. Cbl treatment significantly reduced amyloid plaques in both groups. **C** Levels of perivascular GFAP immunoreactivity expressed as corrected optical density. Cbl treatment significantly reduced levels of astroglial reactivity in both groups. **D** Levels of interstitial GFAP immunoreactivity expressed as corrected optical density. This represents astrogliosis in the neuropil that does not include the vasculature. Cbl treatment significantly reduced astrogliosis in Group II. **E** Levels of CD31 immunoreactivity expressed as corrected optical density. Cbl treatment significantly increased levels of this vascular marker in both groups. **F** Levels of ZO-1 immunoreactivity expressed as corrected optical density. Cbl treatment significantly increased expression of this vascular marker in Group II. For Group I, $n = 6$ tg mice treated with saline and 6 tg mice treated with Cbl. For Group II, $n = 6$ tg mice treated with saline and 6 tg mice treated with Cbl. $* = p < 0.05$ by one-way ANOVA with post-hoc Fisher

(Fig. 3B). This effect was more apparent in the older group of mice, Group II (Fig. 3A, B), where only a few deposits were observed in smaller vascular branches penetrating the cortical neuropil (Fig. 2E, F), hippocampus and thalamus (not shown). Only occasional deposits were observed in the pial surface of these mice (Fig. 2E, F).

Effects of Cbl treatment on neuroinflammation and markers of vascular integrity

To further investigate the effects of Cbl on neuroinflammation and vascular fitness, immunocytochemical studies with antibodies against astroglial, microglial, lymphocytic and vascular markers were performed. In saline-treated mThy1-hAPP751 tg mice no perivascular lymphocytic infiltrates were detected in hematoxylin and eosin (H&E) stained sections (Fig. 4A–C) or in sections stained with CD3 or CD20 (not shown). In contrast, in these mice there was intense perivascular and interstitial (Fig. 4E) microgliosis and astrogliosis (Fig. 3C, D; Fig. 4H) that were more severe in older mice. Cbl treatment resulted in a significant decrease in the levels of perivascular microgliosis (Fig. 4F) and astrogliosis (Fig. 4I) in both groups of mice (Fig. 3C). Cbl treatment also reduced interstitial astrogliosis but this effect was only significant in mice from Group II (Fig. 3D). In the control mice, the antibodies against CD31 (Fig. 4J) and ZO-1 (Fig. 4M) labeled the wall of the vessels of small and intermediate caliber. Compared to controls, in the saline-treated mThy1-hAPP tg mice levels of immunoreactivity for those vascular markers was decreased (Fig. 4K, N). In contrast, Cbl treatment resulted in the amelioration of the vascular alterations with close to control levels of CD31 (Fig. 4L) and ZO-1 (Fig. 4O) immunoreactivity in tg mice. Computer-aided image analysis showed that Cbl treatment rescued the levels of CD31 immunoreactivity in both groups of mice (Fig. 3E). Similar effects were observed for ZO-1 immunoreactivity, however, statistical significance was only obtained for Group II (Fig. 3F).

Effects of Cbl on the subcellular organization of the cerebral vasculature

Ultrastructural analysis of the leptomeningial, neocortical and hippocampal arteries of the saline-treated mThy1-hAPP751 tg mice showed an abundant accumulation of amyloid fibrils in the walls of arterial vessels of small and intermediate caliber (Fig. 5A, B). Amyloid fibrils were found within smooth muscle cells and the elastic lamina disrupting the vascular architecture (Fig. 5A). The vascular amyloid deposits consisted of randomly oriented bundles of fibers measuring approximately 8–10 nm in diameter (Fig. 5B). Furthermore, the basal lamina was thickened and contained focal electrodense deposits (Fig. 5B). In some vessels, the adventitia was expanded by foamy appearing structures containing electrodense vacuoles, phagolysosomes and laminated bodies (Fig. 5C). The pericytes of some of these vessels also contained large lipid droplets (Fig. 5D, E). These alterations were more abundant in the older mice compared to the younger group. Capillaries were relatively well preserved, however vacuolized cellular processes containing laminated structures

were often found around them (Fig. 5F). In contrast, in the vessels of Cbl-treated mThy1-hAPP751 tg mice only occasional amyloid fibrils were found (Fig. 6A–C). The basement membranes displayed relatively normal characteristics and no vacuoles or laminar bodies were found (Fig. 6D, E). The cellular junctions among endothelial cells were preserved and only sporadic electrodense deposits were identified (Fig. 6D, E). Capillaries and pericytes showed normal characteristics (Fig. 6F).

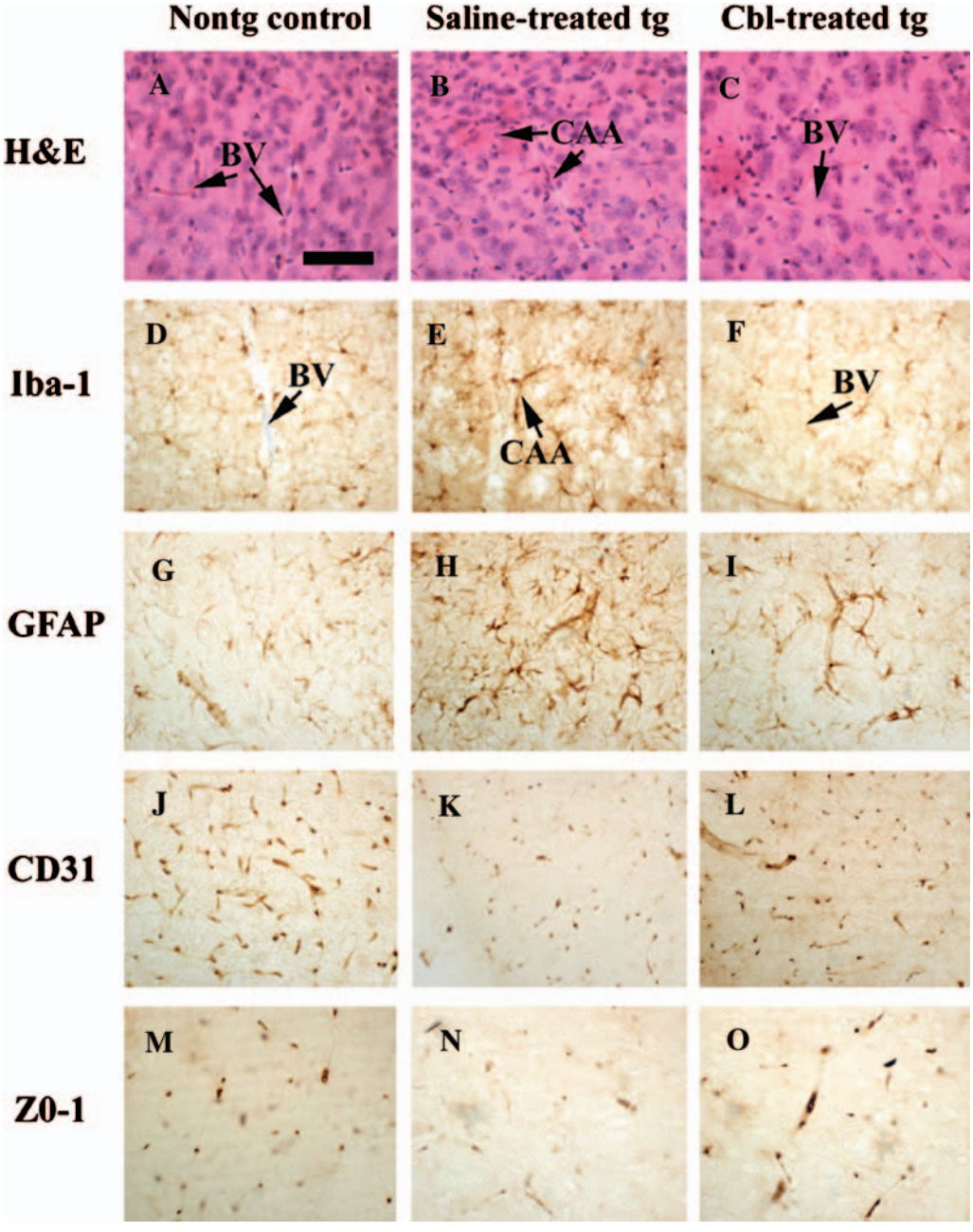

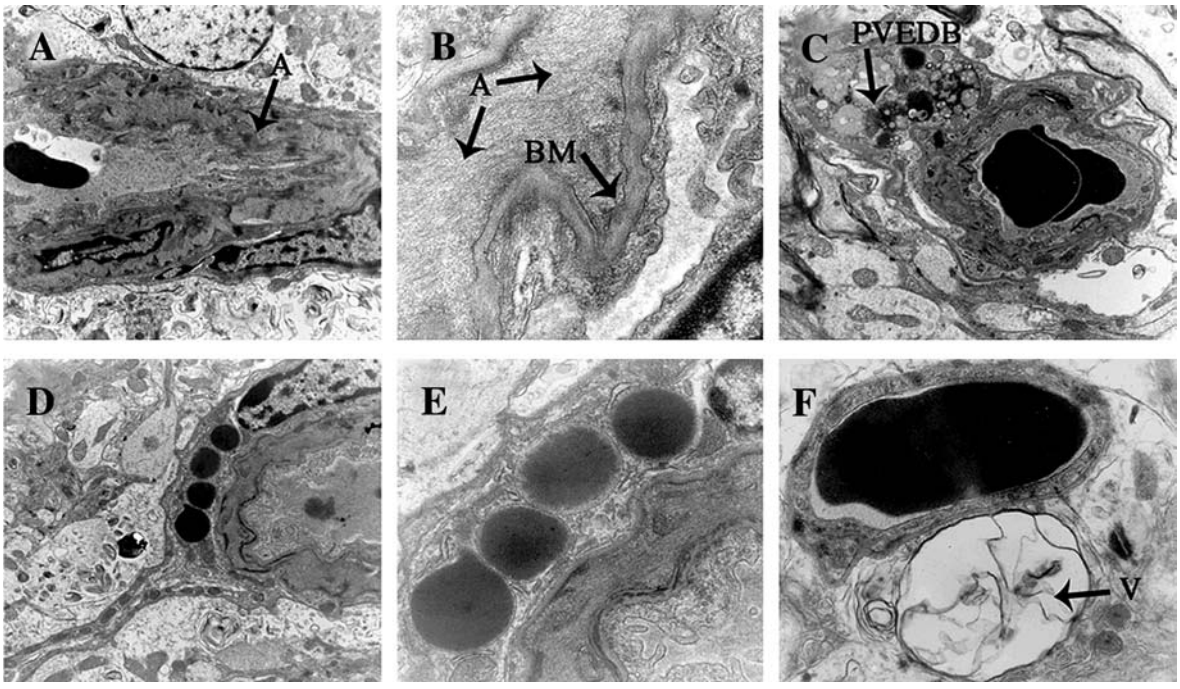

Fig. 5. Ultrastructural analysis of the vasculature in saline-treated mThy1-hAPP751 tg mice. All images are from the frontal cortex of mice from Group II. **A** Low-power view (5000×) of an intermediate caliber vessel displaying abundant amyloid deposition in the media. **B** Higher power view (15000×) of amyloid deposits around the basement membrane and thickening of the membrane. **C** Accumulation of perivascular electrodense and vacuolized bodies (10000×). **D** Intermediate caliber vessel displaying abundant electrodense lipid-like vacuoles in the cytoplasm of pericytes (5000×). **E** Higher power magnification (15000×) of electrodense vacuoles and thickened basement membrane containing electrodense deposits. **F** Vacuolized cellular processes surrounding an otherwise unaffected capillary (10000×). *A* amyloid deposit, *BM* basement membrane, *PVEDB* perivascular electrodense bodies, *V* vacuoles

Fig. 4. Neuropathological and immunocytochemical analysis of the patterns of vascular damage in Cbl and saline-treated mThy1-hAPP751 tg mice and nontg control mice. Images are from the frontal cortex of mice from Group II. Panels **A**–**C** show the microvasculature in sections stained with hematoxylin and eosin (H&E). No inflammatory lymphocytic infiltration is observed in the vessels (arrows) displaying amyloid angiopathy (CAA). Panels **D**–**F** show increased microglial Iba1 immunoreactivity around vessels (arrows) in tg mice treated with saline. In mice treated with Cerebrolysin, there is a decrease in the intensity of this microglial reaction. Panels **G**–**I** show GFAP immunoreactivity demonstrating an increase in astrogliosis around the vessels in tg mice treated with saline and an amelioration of this process in Cbl treated mice. Panels **J**–**L** demonstrate CD31 immunoreactivity showing a decrease in CD31 expression in saline-treated tg mice compared to nontg control and Cbl-treated tg mice. Panels **M**–**O** display ZO-1 immunoreactivity, also displaying a decrease in expression in saline-treated tg mice compared to control and Cbl-treated tg mice. **A**, **D**, **G**, **J**, **M** Nontg control. **B**, **E**, **H**, **K**, **N** Saline-treated tg mouse section. **C**, **F**, **I**, **L**, **O** Cbl-treated tg mouse section. *BV* blood vessel, Bar = 20 μm

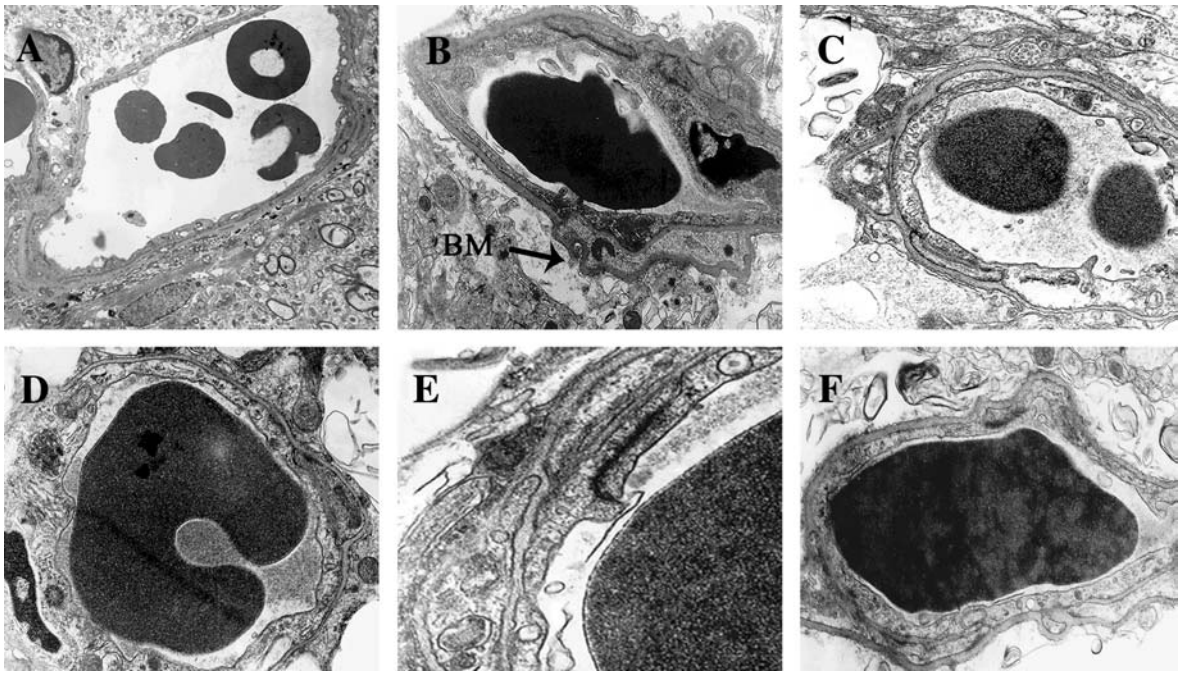

Fig. 6. Ultrastructural analysis of the effects of Cbl on the vasculature of Cbl-treated mThy1-hAPP751 tg mice. All images are from the frontal cortex of mice from Group II. **A** Low-power view (5000×) of a relatively preserved vessel of intermediate caliber. **B**, **C** A vessel of small caliber displays mild thickening of the basement membrane and occasional electrodense deposits but no amyloid deposition, shown at 15000× and 10000×, respectively. **D**, **E** Low (5000×) and higher power (15000×) views, respectively, of small caliber vessels displaying preserved endothelial cell junctions. **F** Unaffected capillary (10000×). *BM* basement membrane

Discussion

The present study showed that Cbl treatment ameliorated the age-associated amyloid deposition and degenerative alterations in the vasculature of mThy1-hAPP751 tg mice. Consistent with the vascular changes that characterize this tg model, previous studies have shown that tg mice overexpressing the London mutant of APP under a similar promoter develop significant CAA that increases with age (Van Dorpe et al., 2000). Consistent with our findings that Cbl ameliorates such alterations, previous studies have shown that Cbl decreases Aβ production in tg mice and decreases the formation of amyloid plaques (Rockenstein et al., 2002, 2003). Cbl might reduce CAA and protect the cerebral vasculature through several mechanisms, including regulation of APP metabolism and by increasing the expression of factors that promote vascular fitness. In this regard, previous studies have shown that Cbl alters the ratio of APP 770/751 to 695, favoring APP processing through non-amyloidogenic pathways that also stimulate synapse formation (Mallory et al., 1999; Rockenstein et al., 2002). In addition, Cbl was capable of reducing total APP expression and production of Aβ1-42 and Aβ1-40 in young mThy1-hAPP751 tg mice (Rockenstein et al., 2002). Since previous studies have shown that both sporadic and familial forms of CAA

appear to be associated with a mild perivascular inflammatory response, it is possible that Cbl might reduce the CAA in tg mice by decreasing this neuroinflammatory reaction (Revesz et al., 2002; Eng et al., 2004).

In fact, an inflammatory response to vascular amyloid has also been noted in a tg model that develops CAA (Winkler et al., 2001; Lee et al., 2003). Consistent with this, in the saline-treated mice, we observed mild to moderate astroglial and microglial reaction around the amyloid containing vessels but no lymphocytic infiltration. Cerebrolysin treatment had some modest effects in reducing this perivascular glial reaction, that could potentially help ameliorate amyloid accumulation. This is of interest because preventing the clinical effects of CAA-related inflammation might have implications for combined therapies using neuroprotective agents such as Cbl and vaccination-based treatment strategies for AD. In this regard, a clinical trial of Aβ vaccination was halted when a small proportion of patients developed meningoencephalitis (Check, 2002). Recent autopsy reports in some of these cases have shown that although a large proportion of amyloid in the brain was removed in these patients, CAA persists and in some cases is associated with a prominent inflammatory reaction (Check, 2002). Thus, therapies targeting amyloid deposition and CAA might require not only the use of anti-amyloid and neuroprotective agents but also anti-inflammatory components.

The present study also showed that Cbl enhanced the expression of vascular markers in the APP tg mice and it is possible that this might be associated with the ability of this trophic compound to enhance vascular function by increasing the expression of Glut-1 (Boado and Pardridge, 1993; Boado, 1996), a ubiquitous transporter that is involved in glucose transport in all vertebrates and its expression is increased upon glucose deprivation (Mueckler et al., 1985; Boado and Pardridge, 1993). The mechanism that leads to enhanced vascular function involves a specific mRNA regulatory element (Boado, 2001). The effects of Cbl on glucose transport have been shown to enhance cerebrovascular circulation (Boado et al., 1999) by regulating steady state levels and enhancing stability of Glut1 mRNA (Boado, 1995). Furthermore, previous studies in stroke patients (Koppi and Barolin, 1998) as well as in animal models of vascular obstruction (Schwab et al., 1997, 1998) have shown that this compound might reduce the size of the infarct and accelerate functional recovery. The relationship between the effects of Cbl on APP processing and Glut-1 expression are unclear, but it is conceivable that similar mRNA stabilizing mechanisms might be involved in promoting APP cleavage through non-amyloidogenic pathways such as the α-secretory pathway that results in the production of a secreted α-APP fragment containing the first 16 aa of Aβ. Thus, the effects of Cbl in the cerebral vasculature are important because they might ameliorate not only the neurodegenerative alterations in AD, but also the frequency of cerebral hemorrhages and microinfarcts often associated with this disease.

In summary, this study showed that Cbl decreased amyloid deposition around the blood vessels, increased the expression of markers of vascular fitness, and ameliorated cerebrovascular deficits in mThy1-hAPP751 tg mice. Taken together, these findings suggest that Cbl might have beneficial effects

in ameliorating cognitive deficits due to cerebrovascular damage in AD and CAA patients by reducing amyloid accumulation around the blood vessels.

Acknowledgments

This study was supported by NIH grants AG18440 and AG5131 and by a grant from EBEWE Pharmaceuticals.

References

Beher D, Wrigley JD, Owens AP, Shearman MS (2002) Generation of C-terminally truncated amyloid-beta peptides is dependent on gamma-secretase activity. J Neurochem 82: 563–575

Bertrand E et al. (2001) A short cytoplasmic domain of the amyloid precursor protein induces apoptosis in vitro and in vivo. Mol Cell Neurosci 18: 503–511

Boado R (1995) Brain-derived peptides regulate the steady state levels and increase stability of the blood-brain-barriel GLUT1 glucose transporter mRNA. Neurosci Lett 197: 179–182

Boado R (1996) Brain-derived peptides increase the expression of a blood-brain barrier GLUT1 glucose transporter reporter gene. Neurosci Lett 220: 53–56

Boado RJ (2001) Amplification of blood-brain barrier GLUT1 glucose transporter gene expression by brain-derived peptides. Neurosci Res 40: 337–342

Boado RJ, Pardridge WM (1993) Glucose deprivation causes posttranscriptional enhancement of brain capillary endothelial glucose transporter gene expression via GLUT1 mRNA stabilization. J Neurochem 60: 2290–2296

Boado RJ, Wu D, Windisch M (1999) In vivo upregulation of the blood-brain barrier GLUT1 glucose transporter by brain-derived peptides. Neurosci Res 34: 217–224

Chartier-Harlin M-C et al. (1991) Early-onset Alzheimer's disease caused by mutations at codon 717 of the β-amyloid precursor protein gene. Nature 353: 844–846

Check E (2002) Nerve inflammation halts trial for Alzheimer's drug. Nature 415: 462

Citron M, Diehl T, Capell A, Haass C, Teplow D, Selkoe D (1996) Inhibition of amyloid beta-protein production in neural cells by the serine protease inhibitor AEBSF. Neuron 17: 171–179

Clark R, Goate A (1993) Molecular genetics of Alzheimer's disease. Arch Neurol 50: 1164–1172

Eng JA, Frosch MP, Choi K, Rebeck GW, Greenberg SM (2004) Clinical manifestations of cerebral amyloid angiopathy-related inflammation. Ann Neurol 55: 250–256

Evin G, Zhu A, Holsinger RM, Masters CL, Li QX (2003) Proteolytic processing of the Alzheimer's disease amyloid precursor protein in brain and platelets. J Neurosci Res 74: 386–392

Francis-Turner L, Valouskova V (1996) Nerve growth factor and nootropic drug Cerebrolysin but not fibroblast growth factor can reduce spatial memory impairment elicited by fimbria-fornix transection: short-term study. Neurosci Lett 202: 1–4

Games D et al. (1995) Alzheimer-type neuropathology in transgenic mice overexpressing V717F β-amyloid precursor protein. Nature 373: 523–527

Goate A et al. (1991) Segregation of a missense mutation in the amyloid precursor protein gene with familial Alzheimer's disease. Nature 349: 704

Haass C et al. (1995) The Swedish mutation causes early-onset Alzheimer's disease by beta-secretase cleavage within the secretory pathway. Nat Med 1: 1291–1296

Kanazawa H, Ohsawa K, Sasaki Y, Kohsaka S, Imai Y (2002) Macrophage/microglia-specific protein Iba1 enhances membrane ruffling and Rac activation via phospholipase C-gamma -dependent pathway. J Biol Chem 277: 20026–20032

Koppi S, Barolin GS (1998) [Use of cerebrolysin in the treatment of ischemic stroke]. Zh Nevrol Psikhiatr Im S S Korsakova 98: 30–33

Lee JM et al. (2003) Matrix metalloproteinase-9 and spontaneous hemorrhage in an animal model of cerebral amyloid angiopathy. Ann Neurol 54: 379–382

Lu DC, Shaked GM, Masliah E, Bredesen DE, Koo EH (2003a) Amyloid beta protein toxicity mediated by the formation of amyloid-beta protein precursor complexes. Ann Neurol 54: 781–789

Lu DC, Soriano S, Bredesen DE, Koo EH (2003b) Caspase cleavage of the amyloid precursor protein modulates amyloid beta-protein toxicity. J Neurochem 87: 733–741

Mallory M, Honer W, Hsu L, Johnson R, Masliah E (1999) In vitro synaptotrophic effects of Cerebrolysin in NT2N cells. Acta Neuropathol 97: 437–446

Maruyama K, Kawamura Y, Asada H, Ishiura S, Obata K (1994) Cleavage at the N-terminal site of Alzheimer amyloid beta/A4 protein is essential for its secretion. Biochem Biophys Res Commun 202: 1517–1523

Masliah E (1999) Transgenic animal models of Alzheimer disease. In: Terry R, Katzman R, Bick K, Sisodia S (eds) Alzheimer disease, 2nd edn. Lippincott, Williams and Wilkins, Philadelphia, pp 245–262

Masliah E, Rockenstein E (2000) Genetically altered transgenic models of Alzheimer's disease. J Neural Transm [Suppl] 59: 175–183

Masliah E, Armasolo F, Veinbergs I, Mallory M, Samuel W (1999) Cerebrolysin ameliorates performance deficits and neuronal damage in apolipoprotein E-deficient mice. Pharmacol Biochem Behav 62: 239–245

Mattson MP (2000) Apoptotic and anti-apoptotic synaptic signaling mechanisms. Brain Pathol 10: 300–312

Mattson MP, Gary DS, Chan SL, Duan W (2001) Perturbed endoplasmic reticulum function, synaptic apoptosis and the pathogenesis of Alzheimer's disease. Biochem Soc Symp: 151–162

Mucke L et al. (2000) High-level neuronal expression of Abeta 1-42 in wild-type human amyloid protein precursor transgenic mice: synaptotoxicity without plaque formation. J Neurosci 20: 4050–4058

Mueckler M et al. (1985) Sequence and structure of a human glucose transporter. Science 229: 941–945

Revesz T et al. (2002) Sporadic and familial cerebral amyloid angiopathies. Brain Pathol 12: 343–357

Rockenstein E, McConlogue L, Tan H, Power M, Masliah E, Mucke L (1995) Levels and alternative splicing of amyloid β protein precursor (APP) transcripts in brains of APP transgenic mice and humans with Alzheimer's disease. J Biol Chem 270: 28257–28267

Rockenstein E, Mallory M, Mante M, Sisk A, Masliah E (2001) Early formation of mature amyloid-b proteins deposits in a mutant APP transgenic model depends on levels of Ab1-42. J Neurosci Res 66: 573–582

Rockenstein E et al. (2002) Effects of Cerebrolysin on amyloid-beta deposition in a transgenic model of Alzheimer's disease. J Neural Transm [Suppl] 62: 327–336

Rockenstein E, Adame A, Mante M, Moessler H, Windisch M, Masliah E (2003) The neuroprotective effects of Cerebrolysin trade mark in a transgenic model of Alzheimer's disease are associated with improved behavioral performance. J Neural Transm 110: 1313–1327

Ruther E, Ritter R, Apecechea M, Freitag S, Windisch M (1994a) Efficacy of Cerebrolysin in Alzheimer's disease. In: Jellinger K, Ladurner G, Windisch M (eds) New trends in the diagnosis and therapy of Alzheimer's disease. Springer, Wien New York, pp 131–141

Ruther E, Ritter R, Apecechea M, Freytag S, Windisch M (1994b) Efficacy of the peptidergic nootropic drug cerebrolysin in patients with senile dementia of the Alzheimer's type (SDAT). Pharmacopsychiatry 27: 32–40

Schwab M, Schaller R, Bauer R, Zwiener U (1997) Morphofunctional effects of moderate forebrain ischemia combined with short-term hypoxia in rats – protective effects of Cerebrolysin. Exp Toxicol Pathol 49: 29–37

Schwab M, Antonow-Schlorke I, Zwiener U, Bauer R (1998) Brain-derived peptides reduce the size of cerebral infarction and loss of MAP2 immunoreactivity after focal ischemia in rats. J Neural Transm [Suppl] 53: 299–311

Sisodia S, Koo E, Beyreuther K, Unterbeck A, Price D (1990) Evidence that β-amyloid protein in Alzheimer's disease is not derived by normal processing. Science 248: 492–494

Van Dorpe J et al. (2000) Prominent cerebral amyloid angiopathy in transgenic mice overexpressing the london mutant of human APP in neurons. Am J Pathol 157: 1283–1298
Van Nostrand WE et al. (2002) Localization of a fibrillar amyloid beta-protein binding domain on its precursor. J Biol Chem 277: 36392–36398
Veinbergs I, Mante M, Mallory M, Masliah E (2000) Neurotrophic effects of Cerebrolysin in animal models of excitotoxicity. J Neural Transm [Suppl] 59: 273–280
Weller RO, Nicoll JA (2003) Cerebral amyloid angiopathy: pathogenesis and effects on the ageing and Alzheimer brain. Neurol Res 25: 611–616
Winkler DT et al. (2001) Spontaneous hemorrhagic stroke in a mouse model of cerebral amyloid angiopathy. J Neurosci 21: 1619–1627
Wyss-Coray T et al. (1997) Amyloidogenic role of transforming growth factor β1 in transgenic mice and Alzheimer's disease. Nature 389: 603–606
Wyss-Coray T, Lin C, Sanan DA, Mucke L, Masliah E (2000) Chronic overproduction of transforming growth factor-beta1 by astrocytes promotes Alzheimer's disease-like microvascular degeneration in transgenic mice. Am J Pathol 156: 139–150

Authors' address: Dr. E. Masliah, Department of Neurosciences, University of California, San Diego, La Jolla, CA 92093-0624, USA, e-mail: emasliah@ucsd.edu